Efficient backcalculation procedure for asphalt pavements using the Finite Element Method

Elias S. Barroso[1], José L. F. Oliveira[1], Evandro Parente Jr. [1], Lucas F. A. L. Babadopulos[1], Juceline B. S. Bastos[2]

[1]*Departamento de Engenharia Estrutural e Construção Civil, Universidade Federal do Ceará*
Campus do Pici, Bloco 728, 60440-900, Ceará, Brasil
elias.barroso@gmail.com, lucasfer1227@alu.ufc.br, evandro@ufc.br, babadopulos@ufc.br
[2]*Instituto Federal de Educação, Ciência e Tecnologia do Ceará*
Campus Fortaleza, Av. Treze de Maio, 2081, 60040-531, Ceará, Brasil
juceline.santos@ifce.edu.br

Abstract. Backcalculation is a procedure used to estimate stiffness properties (resilient modulus) of asphalt pavement layers through non-destructive tests. The resilient modulus of each pavement layer is adopted as the one that produces the simulated deflections closest to the deflections obtained in field tests. This paper presents an efficient backcalculation approach based on the minimization of the sum of squared errors between the measured field deflections and deflections obtained using an axisymmetric linear elastic layered model for the pavement with finite and infinite elements. The resulting nonlinear least squares problem is solved using the Gauss-Newton (GN) and the Levenberg–Marquardt (LM) methods. The gradients of deflections with respect to the material parameters used by the optimization methods are computed accurately and efficiently by the finite element code. The two methods are compared in terms of accuracy, robustness, and computational efficiency for pavement structures with different characteristics.

Keywords: Backcalculation, Asphalt Pavements, Finite Element Method, Nonlinear Least Squares.

1 Introduction

Backcalculation is a procedure used to estimate stiffness properties (resilient modulus) of asphalt pavement layers through non-destructive tests, as the Falling Weight Deflectometer (FWD) and the Benkelman beam (Scimemi et al., [1]; Kheradmandi and Modarres, [2]). This procedure is important to assess the quality of a pavement structure during its construction and/or to monitor its condition during its lifespan.

In the FWD test, an impulse load due to the falling weight is imposed on the pavement surface. This load is transmitted to the pavement through a loading plate. Sensors and geophones located at several radial offsets are used to measure the surface deflections. The measurement made by each geophone represents the deflection of the pavement structure at a particular location. Peak deflection is measured by the geophone directly below the load application point and deflections are smaller for more distant geophones (Huang, [3]).

Using the measured deflection basins, it is possible to determine the equivalent resilient moduli of the pavement layers through the backcalculation process. This process considers several theoretical assumptions including static loading, material continuity, layer homogeneity, and linear elastic behavior.

Pavement deflections due to the applied loads depend on layer thicknesses and material stiffness properties (moduli and Poisson's ratios). However, it is generally accepted that the layers' thicknesses are known and only the material properties need to be evaluated by backcalculation. Furthermore, it is assumed that the Poisson's ratio presents a small influence on pavement response and its value can be defined based only the material type of each layer. Therefore, only the resilient modulus (i.e. modulus of elasticity) of each layer needs to be backcalculated.

Assuming that the pavement response is linear elastic, the deflections at the measurement points (geophones) due to the applied FWD load can be computed using the Finite Element Method (FEM) (Cook et al., [4]) or the Multilayered Elastic Theory (MLET) (Huang, [3]). Thus, the resilient modulus of the pavement layers can be evaluated by minimizing the difference between the simulated and the measured field deflections.

This paper presents an efficient backcalculation approach based on the minimization of the sum of squared errors between the simulated and the measured deflections, obtained using an accurate and efficient FE model. The resulting nonlinear least squares problem is solved using the Gauss-Newton and the Levenberg–Marquardt methods. The gradients of deflections with respect to the material parameters used by the optimization methods are computed accurately and efficiently by the finite element code. The two methods are compared in terms of accuracy, robustness, and computational efficiency for pavement structures with different characteristics.

2 Backcalculation of pavement properties

The FWD load (F) is applied at a circular loading plate of radius (r). Considering that the resulting pressure applied to the pavement is uniform ($p = F/\pi r^2$) and that the deflected region is much smaller than the pavement dimensions, the pavement responses can be evaluated using an axisymmetric model, which is much more efficient than a 3D one. Therefore, in this work the simulated deflections are computed using an axisymmetric FE model with a mesh composed of quadratic finite (Q8) and infinite (L6) elements (Silva et al., [5]), as shown in Figure 1. Numerical analyses are carried out using the CAP3D program (Holanda et al., [6]). The use of infinite elements allows to reduce the number of finite elements and improves the displacements accuracy (Silva et al., [5]). The mesh generation algorithm ensures that there is a node at the position of each geophone.

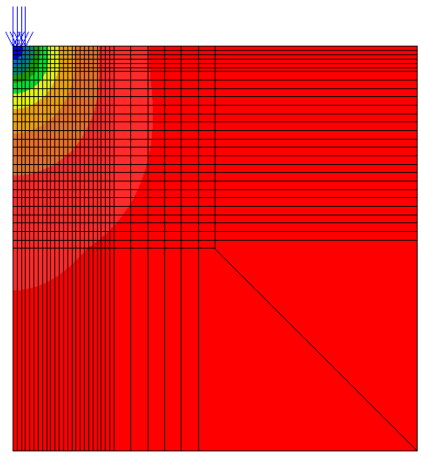

Figure 1. Axisymmetric mesh used for backcalculation.

In FEM, the nodal displacement vector ($\mathbf{u}$) is computed solving the linear system of equilibrium equations:

$$\mathbf{K}\,\mathbf{u} = \mathbf{f} \tag{1}$$

where $\mathbf{K}$ is the global stiffness matrix and $\mathbf{f}$ is the external load vector. The global stiffness of the FE model is assembled by the classical direct stiffness approach summing up the element stiffness matrices ($\mathbf{K}_e$):

$$\mathbf{K}_e = \int_{V_e} \mathbf{B}^T \mathbf{C}\,\mathbf{B}\,dV, \quad \mathbf{C} = E\,\mathbf{A}(\upsilon) \tag{2}$$

where V_e is the element volume, $\mathbf{B}$ is the strain-displacement matrix, and $\mathbf{C}$ is the elastic constitutive matrix for the axisymmetric model, E is the modulus of elasticity, and $\mathbf{A}$ is a matrix depending only on the Poisson's ratio (υ) (Cook et al., [4]).

This FEM model can be used to evaluate the deflections due to the FWD loading, provided that the pavement geometry and material properties are known. In this work, it is assumed that the thickness (h) and Poisson's ratio (υ) of each layer is known and only the modulus of elasticity (E) needs to be backcalculated. Considering a pavement with *n* layers and a FWD device with *m* geophones, the backcalculation problem can be written as:

$$\min_{\mathbf{p}\,\in\,\mathbb{R}^n} f(\mathbf{p}) = \frac{1}{2}\sum_{i=1}^{m}\left(\hat{d}_i - d_i\right)^2 = \frac{1}{2}\sum_{i=1}^{m} r_i^2 = \frac{1}{2}\mathbf{r}^T\mathbf{r}, \quad n \le m \tag{3}$$

where $\hat{d}_i$ are the simulated deflections (FEM), d_i are the measured deflections (FWD), **r** is the residual vector and

$$\mathbf{p} = [E_1, \cdots, E_n]^T \tag{4}$$

is the vector of unknown parameters. Equation (3) corresponds to the classical Nonlinear Least Squares (NLS) problem (Madsen et al., [7]; Nocedal and Wright, [8]) which can be solved using different algorithms. The Gauss-Newton and the Levenberg–Marquardt methods are applied in this work.

2.1 Gauss-Newton

Gauss-Newton method is obtained by the application of the Newton method to the NLS problem. The Newton method is based on a quadratic approximation of the function to be minimized:

$$f(\mathbf{p}_{k+1}) \approx f(\mathbf{p}_k) + {\mathbf{d}_k}^T \nabla f(\mathbf{p}_k) + \tfrac{1}{2}{\mathbf{d}_k}^T \mathbf{H}(\mathbf{p}_k)\,\mathbf{d}_k \tag{5}$$

where *k* is the iteration number, **d** is search direction, ∇f is the gradient, and $\mathbf{H} = \nabla^2 f$ is the Hessian matrix. The search direction (**d**) at each iteration *k* is computed minimizing the approximate quadratic function:

$$\nabla f(\mathbf{p}_{k+1}) \approx \nabla f(\mathbf{p}_k) + \mathbf{H}(\mathbf{p}_k)\mathbf{d}_k = \mathbf{0} \quad \Longrightarrow \quad \mathbf{d}_k = -(\mathbf{H}_k)^{-1}\,\nabla f_k \tag{6}$$

Finally, the new estimate of the parameter (**p**) vector can be obtained using:

$$\mathbf{p}_{k+1} = \mathbf{p}_k + \alpha\mathbf{d}_k \tag{7}$$

where α is the step size along the search direction, obtained by a line search algorithm (Nocedal and Wright, [8]).

Using exact gradient and Hessian, the Newton method presents local quadratic convergence. On the other hand, global convergence is not assured, but its robustness can be greatly improved by line searches. It can be shown that $\mathbf{d}_k$ is a descent direction, provided that $\mathbf{H}_k$ is positive definite (Nocedal and Wright, [8]). Thus, a simple backtracking algorithm is used here, where $\alpha = 1$ is adopted as the initial step size and the descent condition

$$f(\mathbf{p}_k + \alpha\mathbf{d}_k) < f(\mathbf{p}_k) \tag{8}$$

is tested. If this condition is satisfied, the step size is accepted, otherwise it is halved ($\alpha = \alpha/2$) and the test is repeated. This approach allows for a unit step size at the solution, which is a condition for quadratic convergence.

For NLS problems described by Eq. (3), the gradient and Hessian matrix are given by

$$\nabla f = \mathbf{r}^T\mathbf{J} \qquad \text{and} \qquad \mathbf{H} = \mathbf{J}^T\mathbf{J} + \sum_{i=1}^{m} r_i\,\nabla {r_i}^2 \tag{9}$$

where **J** is the Jacobian matrix:

$$\mathbf{J} = [J_{ij}] = \left[\frac{\partial r_i}{\partial p_j}\right] = \left[\frac{\partial \hat{d}_i}{\partial p_j}\right] \tag{10}$$

In several NLS problems, the second term of the Hessian matrix is small close to the solution, either because the residual is very small or the Jacobian is affine with respect to the model parameters (Nocedal and Wright, [8]). The GN method is obtained neglecting this term and considering $\mathbf{H} \approx \mathbf{J}^T\mathbf{J}$. Thus, the search direction at each iteration is computed by solving the linear system:

$$\left({\mathbf{J}_k}^T\mathbf{J}_k\right)\mathbf{d}_k = -\,{\mathbf{J}_k}^T\mathbf{r}_k \tag{11}$$

The iterations can be stopped when:

$$|f(\mathbf{p}_k)| < \varepsilon_1 \quad \text{or} \quad |\nabla f(\mathbf{p}_k)| < \varepsilon_2 \tag{12}$$

where ε_1 and ε_2 are user defined tolerances.

The convergence rate of GN method depends on how close $\mathbf{J}^T\mathbf{J}$ approximates the true Hessian and can be close to quadratic. On the other hand, failure can occur if the approximate Hessian is singular. Furthermore, when the initial point $\mathbf{p}_0$ is far from the solution, the quadratic approximation may be not accurate, which generates poor search directions, leading to slow improvement or divergence.

2.2 Levenberg–Marquardt

The Levenberg–Marquardt (LM) method (Madsen et al., [7]; Nocedal and Wright, [8]) was proposed as a more robust alternative to the GN method. This method is based on a modified form of Eq. (11):

$$\left(\mathbf{J}_k{}^T\mathbf{J}_k + \lambda\mathbf{I}\right)\mathbf{d}_k = -\mathbf{J}_k{}^T\mathbf{r}_k \tag{13}$$

The damping parameter ($\lambda > 0$) ensures that the coefficient matrix is positive definite, generating a descent search direction $\mathbf{d}_k$. For large values of λ, $\mathbf{d}_k \approx -\nabla f\,/\,\lambda$ is a short step in the steepest descent direction ($-\nabla f$), which is a good option if the current iterates $\mathbf{p}_k$ is far from the solution. Finally, if λ very small, then Eq. (12) reduces to Eq. (11), generating the same search direction then the GN method, which is good in the final iterations when $\mathbf{p}_k$ is close to the solution, and GN can present quadratic convergence. Since λ controls not only the search direction but also the step size, the LM algorithm is used without line search.

The main idea of the LM method is to begin with a relatively large factor λ. If $\mathbf{d}_k$ provides a good decrease in $f(\mathbf{p}_k + \mathbf{d}_k)$, the new step ($\mathbf{p}_{k+1} = \mathbf{p}_k + \mathbf{d}_k$) is accepted and λ is decreased. Otherwise, this step is not accepted and λ is increased. Several approaches have been proposed in the literature to update the damping factor. In this work, we adopt the approach proposed by Madsen et al. (2004), where the initial factor is given by:

$$\lambda_0 = \tau \max(\mathbf{J}_0{}^T\mathbf{J}_0) \tag{14}$$

with $\tau > 0$. After each iteration, the damping factor is updated according to the gain ratio:

$$\rho = \frac{f(\mathbf{p}_k) - f(\mathbf{p}_k + \mathbf{d}_k)}{L(\mathbf{p}_k) - L(\mathbf{p}_k + \mathbf{d}_k)} \quad \Rightarrow \quad \rho = \frac{f(\mathbf{p}_k) - f(\mathbf{p}_k + \mathbf{d}_k)}{\frac{1}{2}\mathbf{d}_k{}^T\left(\lambda\mathbf{d}_k - \mathbf{J}_k{}^T\mathbf{r}_k\right)} \tag{15}$$

where the denominator L is the gain predicted by Eq. (5), which is guaranteed to be positive (Madsen et al., 2004). After that, the damping factor is updated according to

$$\begin{cases} \lambda = \lambda \max\left\{\frac{1}{3}, 1 - (2\rho - 1)^3\right\};\ \ \kappa = 2, & \text{if } \rho > 0 \\ \lambda = \lambda\,\kappa;\ \kappa = 2\,\kappa, & \text{if } \rho \le 0 \end{cases} \tag{16}$$

The factor κ is initialized as $\kappa = 2$. According to this scheme, the damping factor λ varies smoothly along the iterations, being multiplied by 2 as ρ approaches 0, kept almost constant for $0.25 \le \rho \le 0.75$, and being divided by 3 for $\rho \ge 1$. Furthermore, negative gain ratios lead to a quick increase of the damping factor. The convergence can be checked using Eq. (12).

2.3 Sensitivity analysis

The derivatives of nodal displacements required in Eq. (10) can be computed by differentiation of Eq. (11) with respect to parameter p_j:

$$\frac{\partial\mathbf{K}}{\partial p_j}\mathbf{u} + \mathbf{K}\frac{\partial\mathbf{u}}{\partial p_j} = \frac{\partial\mathbf{f}}{\partial p_j} \quad \Rightarrow \quad \mathbf{K}\frac{\partial\mathbf{u}}{\partial p_j} = \mathbf{h}_j \tag{17}$$

where $\mathbf{h}_j$ the pseudo-load vector is given by

$$\mathbf{h}_j = \frac{\partial\mathbf{f}}{\partial p_j} - \frac{\partial\mathbf{K}}{\partial p_j}\mathbf{u} \tag{18}$$

It is important to note that $\partial\mathbf{f}\,/\,\partial p_j = \mathbf{0}$, since the external load vector does not depend on the material parameters. Furthermore, $\partial\mathbf{K}\,/\,\partial p_j$ can be exactly computed using finite differences, since $\mathbf{K}$ depends linearly on the modulus of elasticity (E), as shown in Eq. (2).

This procedure to exactly evaluate the displacement derivatives required by the NLS algorithms was implemented in CAP3D program. It requires the solution of an additional linear system for each model parameter.

Since the matrix **K** was already factored to solve Eq. (1), the additional computational cost is small in comparison with a standard FE analysis. The column j of the Jacobian matrix (**J**) is assembled using the components of $\partial \mathbf{u} / \partial p_j$ corresponding to vertical displacements of the nodes located at the geophones.

3 Numerical examples

The first example corresponds to a manufactured solution used to validate the formulation and implementation of the numerical methods described in the previous section. The geometric and stiffness parameters are presented in Table 1 and the corresponding deflection basin (Table 2) was determined by FEM using the same mesh adopted for backcalculation. It is worth mentioning that the radius and force used in these examples were 15 cm and 41 kN. This example is inspired in the three-layer pavement presented in Reddy et al. [9] and Scimemi et al. [1], but using the pavement data presented by Silva et al [5].

Table 1. Example 1 – Pavement structure.

Layers	Thickness (m)	Modulus of elasticity (MPa)	Poisson's ratio
Asphalt coating	0.10	3500	0.35
Base	0.20	350	0.30
Subgrade	7.50	100	0.40

Table 2. Example 1 – Deflection basin.

Distance (cm)	0	20	30	45	60	90	120
Deflection (μm)	471.75900	369.75346	307.95301	239.01464	190.47159	129.27643	94.61561

The NLS algorithms were started from different points to assess their accuracy, efficiency, and robustness. The tolerances for convergence, defined according to Eq. (12), were ε_1 = 10^{-6} and ε_2= 10^{-8}. The Levenberg-Marquardt method was used with $\tau = 1$. The obtained results, elapsed time, and number of iterations are presented in Table 3 (Gauss-Newton) and Table 4 (Levenberg–Marquardt). The machine used for backcalculation process has an Intel Core i5-8265U processor with 8 Gb RAM and 128 Gb SSD.

Table 3. Example 1 – Results of Gauss-Newton method.

Initial Modulus (MPa)			Final Modulus (MPa)			Time (s)	#Iter
Layer 1	Layer 2	Layer 3	Layer 1	Layer 2	Layer 3		
3500.0	350.00	100.00	3500.0	350.00	100.00	0.6304	-
4000.0	300.00	75.000	3500.0	350.00	100.00	5.8945	4
2500.0	500.00	50.000	3500.0	350.00	100.00	7.8890	5
2000.0	200.00	150.00	3500.0	350.00	100.00	7.3730	5
5000.0	500.00	200.00	3500.0	350.00	100.00	5.9150	4
6000.0	1000.0	400.00	3500.0	350.00	100.00	8.4930	6

Table 4. Example 1 – Results of Levenberg–Marquardt method.

Initial Modulus (MPa)			Final Modulus (MPa)			Time (s)	#Iter
Layer 1	Layer 2	Layer 3	Layer 1	Layer 2	Layer 3		
3500.0	350.00	100.00	3500.0	350.00	100.00	0.75230	-
4000.0	300.00	75.000	3500.0	350.00	100.00	21.342	18
2500.0	500.00	50.000	3500.0	350.00	100.00	25.306	20
2000.0	200.00	150.00	3499.9	350.01	100.00	20.767	16
5000.0	500.00	200.00	3500.2	349.98	100.00	16.892	14
6000.0	1000.0	400.00	3500.3	349.98	100.00	24.565	23

As expected, the number of iterations decreases when the initial point is closer to the solution and no iterations are carried out when the exact solution is used as the starting point. The results show that both algorithms are accurate and robust, finding the correct solution from all starting points considered in this work. However, with respect to computational efficiency, the Gauss-Newton method was superior, requiring fewer iterations for all starting points.

The second example corresponds to the application of the NLS algorithms to the backcalculation of three different asphalt pavements encountered in Brazilian roads:

- Pavement 2: well sized structure with CAP 50/70 asphalt coating (E = 3243 MPa, h = 5 cm, ν = 0.35), simple graded gravel (E = 381 MPa, h = 15 cm, ν = 0.3) in the base, a clayey soil (E = 250 MPa, h = 15 cm, ν = 0.3) in the sub-base, and a silty soil (E = 189 MPa, ν = 0.40) in the subgrade.
- Pavement 3: semi-rigid pavement, with graded gravel treated with cement used (E = 4500 MPa) in the base, overcoming the stiffness of the upper layer.
- Pavement 4: defective structure, with a poorly compaction of the sub-base, reducing its stiffness (E = 90 MPa) and making it smaller than the stiffness of the subgrade.

These pavements are more complex than the previous one since they present four layers. As in the previous example, the exact deflection basin was determined by FEM using the same mesh adopted for backcalculation. The resulting deflection basins for the three pavements are presented in Table 5. The radius and force used in this example were 15 cm and 41 kN. The same algorithm parameters of the previous example were adopted here.

The same starting point (E_1 = 2000 MPa, E_2 = 200 MPa, E_3 = 200 MPa, E_4 = 150 MPa) was used for all pavements. The obtained results, elapsed time, and number of iterations are presented in Table 6 (Gauss-Newton) and Table 7 (Levenberg–Marquardt).

Table 5. Example 2 – Deflection basins.

Distance (cm)	0	20	30	45	60	90	120
Deflection (μm) - Pav. 2	441.445	268.638	191.629	133.363	101.277	66.7199	49.0573
Deflection (μm) - Pav. 3	223.192	182.327	159.393	129.566	105.198	71.2286	51.2071
Deflection (μm) - Pav. 4	541.040	341.055	241.568	156.678	109.807	66.0115	47.7723

Table 6. Example 2 – Results of Gauss-Newton method.

Layer	Pavement 2		Pavement 3		Pavement 4	
	E (MPa)	#Iter (time)	E (MPa)	#Iter (time)	E (MPa)	#Iter (time)
Asphalt coating (5 cm)	3243.0	4 (5.53 s)	3243.0	8 (9.91 s)	3243.0	5 (8.40 s)
Base (15 cm)	381.00		4500.0		381.00	
Sub-base (15 cm)	250.00		250.00		90.000	
Subgrade (-)	189.00		189.00		189.00	

Table 7. Example 2 – Results of Levenberg–Marquardt method.

Layer	Pavement 2		Pavement 3		Pavement 4	
	E (MPa)	#Iter (time)	E (MPa)	#Iter (time)	E (MPa)	#Iter (time)
Asphalt coating (5 cm)	3243.0	19 (24.5 s)	3242.7	27 (33.3 s)	3242.3	19 (30.8 s)
Base (15 cm)	381.00		4500.1		381.03	
Sub-base (15 cm)	250.00		250.01		89.996	
Subgrade (-)	189.00		189.00		189.00	

It should be noted that both algorithms obtained the correct results for all pavements, including Pavement 3 with a stiffer base and Pavement 4 with a poorly compacted sub-base. Therefore, they can be used to assess the quality of a pavement structure and detect construction problems through the nondestructive FWD tests. However, once again, the Gauss-Newton method was superior, requiring fewer iterations for the three different pavement structures considered in this work.

4 Conclusions

This paper presented a backcalculation procedure based on the use of nonlinear least squares (NLS) algorithms to find the elasticity moduli of the pavement layers that best fit the deflections measured in field tests. The numerical model is based on the Finite Element Method and consists of a mixed mesh of finite and infinite quadratic elements. The NLS problem is solved using the Gauss-Newton method with line search and the Levenberg–Marquardt algorithm. The NLS problem is solved efficiently, using the exact derivatives of the finite element deflections to compute the Jacobian matrix.

The effectiveness of the proposed backcalculation procedure was assessed using the method of manufactured solutions, where the measured deflections are obtained numerically, and the number and locations of the deflection measures are the same as used in standard FWD equipment. The results for a pavement with three layers show that both alternatives (GN and LM) are capable to find the correct layer properties for many initial points with varying distances from the problem solution.

The same methodology is applied again in a set of 3 pavements typically observed in Brazillian roads. These pavements have four layers, and the material properties are set to reproduce a representative flexible pavement well-designed, a semi-rigid pavement, and a defective pavement structure. In all the cases, both algorithms predicted the correct material properties. Therefore, both algorithms can be used to perform the backcalculation of pavement properties, which is an important tool to assess the quality of a pavement structure and detect construction problems through nondestructive FWD tests.

The GN method outperformed the LM method in terms of number of iterations and execution time for all examples considered in this work. The excellent performance of GN shows that the approximation of the Hessian matrix did not affect its performance in the problems discussed here. However, further studies need to be carried out to assess its performance for actual FWD data where the fitting errors are not necessarily close to zero. With respect to LM, its well known that its convergence rate depend on the adopted damping update scheme. Since there are several variants presented in the literature, it is important to perform a comprehensive assessment of behavior of these variants for the backcalculation of pavement properties. Moreover, it is important to study the presence of local minima. Furthermore, box constraints can be considered to improve the robustness of the backcalculation procedure.

The effectiveness of the proposed backcalculation procedure will be further investigated considering different starting points and deflection basins with varying noise to reproduce errors observed in actual FWD tests. Finally, we also intend to expand this study to include examples using actual field data.

Acknowledgements. The authors gratefully acknowledge the financial support provided by DNIT (Departamento Nacional de Infraestrutura de Transportes), FUNCAP (Fundação Cearense de Apoio ao Desenvolvimento Científico e Tecnológico), and CNPq (Conselho Nacional de Desenvolvimento Científico e Tecnológico).

Authorship statement. The authors hereby confirm that they are the sole liable persons responsible for the authorship of this work, and that all material that has been herein included as part of the present paper is either the property (and authorship) of the authors, or has the permission of the owners to be included here.

References

[1] G. F. Scimemi, T. Turetta, C. Celauro, "Backcalculation of airport pavement moduli and thickness using the Lévy Ant Colony Optimization Algorithm". *Construction and Building Materials*, vol. 119, pp. 288-295, 2016.

[2] N. Kheradmandi and A. Modarres, "Precision of back-calculation analysis and independent parameters-based models in estimating the pavement layers modulus-Field and experimental study". *Construction and Building Materials*, vol. 171, pp. 598-610, 2018.

[3] Y. H. Huang. *Pavement Analysis and Design*, 2nd Edition, Pearson Prentice Hall, 2004.

[4] R. D. Cook, D. S. Malkus, M. E. Plesha, R. J. Witt. *Concepts and applications of finite element analysis*. 4th Edition, John Wiley & Sons, 2002.

[5] S. A. T. Silva, P. J. F. Vidal, A. S. Holanda, E. Parente Jr., "Análise viscoelástica de pavimentos asfálticos utilizando elementos finitos e infinitos". *Transportes*, v. 21, n. 3, pp. 5-13, 2014.

[6] A. S. Holanda, E. Parente Jr., T. D. P. Araújo, L. T. B. Melo, F. Evangelista Jr., F.; J. B. Soares, "An Object-Oriented System for Finite Element Analysis of Pavements". In: Proceeding of III European Conference on Computational Mechanics (ECCM-2006), p. 1-17, 2006.

[7] K. Madsen, H. B. Nielsen, O. Tingleff, "Methods for non-linear least squares problems", Technical University of Denmark, 2nd Edition, 2004.

[8] J. Nocedal and S. J. Wright. *Numerical Optimization*. 2nd Edition, Springer, 2006.

[9] M. A. Reddy, K.S. Reddy, B. B. Pandey, "Selection of genetic algorithm parameters for backcalculation of pavement moduli", *International Journal of Pavement Engineering*, vol. 5, n. 2, pp. 81–90, 2004.